PROCEEDINGS OF SCIENCE

Review of prospects for $H^{\pm}$ in SUSY models in view of flavour and dark matter results

Farvah Mahmoudi*
CERN Theory Division, CH-1211 Geneva 23, Switzerland
Clermont Université, Université Blaise Pascal, CNRS/IN2P3, LPC, BP 10448, F-63000 Clermont-Ferrand, France
E-mail: mahmoudi@in2p3.fr

We will review the implications of the recent results from flavour physics and dark matter searches on the charged Higgs boson properties. The results will be presented first for the two Higgs doublet model, and next for several MSSM scenarios. We show that combining the flavour and dark matter constraints with those from the Higgs and SUSY searches at the LHC, results in strong constraints on the charged Higgs boson mass.

Prospects for Charged Higgs Discovery at Colliders
October 8-11, 2012
Uppsala University Sweden

*Speaker.

PoS(CHARGED 2012)016

1. Introduction

Search for supersymmetry (SUSY) is the main focus of beyond the Standard Model (BSM) searches in both ATLAS and CMS experiment. No signal has been observed so far and strong limits have been obtained by these experiments in particular in the constrained SUSY scenarios [1, 2]. On the other hand, indirect searches for new physics are being carried out in the flavour and dark matter sectors. Precision flavour physics observables are very sensitive to the presence of new particles in the virtual states, and can probe sectors inaccessible to the direct searches in the case new particles are too heavy to be produced directly. Complementary information can also be obtained from the study of the properties of the dark matter candidate. While in the absence of new signals, direct searches are pushing the limits towards larger mass values, indirect searches can add to the picture substantially and the interplay between the three sectors can allow us to investigate efficiently the SUSY parameter space.

This is an exciting and peculiar time for all these sectors. From the collider side, the LHC experiments are finally running and providing results in an unprecedented energy domain, the discovery of a new boson in ATLAS and CMS experiments has been confirmed, and there are many ongoing searches for new physics signals. From the flavour physics part, the long awaited $B_s \to \mu^+\mu^-$ decay has been observed for the first time and the LHCb experiment has also a very rich BSM program. In the dark matter sector, the Planck cosmological results will be soon released, and we are the witnesses of impressive progress in the sensitivity of dark matter direct detection experiments.

In the following we review the constraints on the SUSY parameters in view of the flavour and dark matter results, and compare the results to those from direct Higgs and SUSY searches at the LHC, and discuss the implications and prospects for the charged Higgs boson.

2. Flavour sector

The theoretical framework for studying the flavour observables is rather complicated as one has to face a multi-scale problem, where we have to consider simultaneously the new physics scale, the scale of electroweak interactions, QCD interactions and hadronic effects. A practical solution to deal with the different involved scales is to use the effective field theory approach where the low and high energy effects are separated using the Operator Product Expansion method. In other word, the heavier degrees of freedom (t, W, Z) are integrated out while the light quarks and gluons are still kept as dynamical particles. This leads to the following effective Hamiltonian:

$$\mathscr{H}_{\text{eff}} = -\frac{4G_F}{\sqrt{2}} V_{tb}V_{ts}^* \Big(\sum_{i=1\cdots 10,S,P} \big(C_i(\mu)\mathscr{O}_i(\mu) + C_i'(\mu)\mathscr{O}_i'(\mu)\big)\Big) \tag{2.1}$$

where C_i are the Wilson coefficients incorporating physics at short distance which are calculated perturbatively, and $\mathscr{O}_i$ are the local operators representing the long distance part. This formalism is very powerful as it can be extended to New Physics easily, through additional contributions to the Wilson coefficients or additional operators.

The Wilson coefficients are calculated by requiring matching between the full and effective theory results at the μ_W scale, then evolved to the μ_b scale, which is the relevant scale for B physics

Observable	Experiment	SM prediction [6]
$\mathrm{BR}(B_s \to \mu^+\mu^-)$	$(3.2\,^{+1.4}_{-1.2}\,^{+0.5}_{-0.3}) \times 10^{-9}$ [3]	$(3.53 \pm 0.38) \times 10^{-9}$
$\langle dBR/dq^2(B \to K^*\mu^+\mu^-)\rangle_{q^2\in[1,6]\mathrm{GeV}^2}$	$(0.42 \pm 0.04 \pm 0.04) \times 10^{-7}$ [4]	$(0.47 \pm 0.27) \times 10^{-7}$
$\langle A_{FB}(B \to K^*\mu^+\mu^-)\rangle_{q^2\in[1,6]\mathrm{GeV}^2}$	$-0.18 \pm 0.06 \pm 0.02$ [4]	-0.06 ± 0.05
$q_0^2(A_{FB}(B \to K^*\mu^+\mu^-))$	$4.9^{+1.1}_{-1.3}\,\mathrm{GeV}^2$ [4]	$4.26 \pm 0.34\,\mathrm{GeV}^2$
$\langle F_L(B \to K^*\mu^+\mu^-)\rangle_{q^2\in[1,6]\mathrm{GeV}^2}$	$0.66 \pm 0.06 \pm 0.04$ [4]	0.72 ± 0.13
$\mathrm{BR}(B \to X_s\gamma)$	$(3.43 \pm 0.21 \pm 0.07) \times 10^{-4}$ [5]	$(3.08 \pm 0.24) \times 10^{-4}$
$\Delta_0(B \to K^*\gamma)$	$(5.2 \pm 2.6) \times 10^{-2}$ [5]	$(8.0 \pm 3.9) \times 10^{-2}$
$\mathrm{BR}(B_u \to \tau\nu_\tau)$	$(1.14 \pm 0.23) \times 10^{-4}$ [5]	$(1.15 \pm 0.29) \times 10^{-4}$

Table 1: Experimental results for the most important rare decays and updated SM predictions.

calculations, using the renormalisation group equations. To compute the amplitudes, one needs to calculate the hadronic matrix elements which are described in terms of hadronic quantities, *i.e.* decay constants and form factors. These quantities are usually the most important source of uncertainty in the calculations.

The most constraining flavour observables for SUSY are the rare decays $b \to s\gamma$, $B_s \to \mu^+\mu^-$ and $B_u \to \tau\nu_\tau$. Other relevant decays are $B \to K^*\mu^+\mu^-$, $B \to K^*\gamma$, $B \to D\tau\nu_\tau$, $D_s \to \tau\nu_\tau$ and $K \to \mu\nu_\mu$. Table 1 summarises the theory predictions and experimental results for these observables. The constraints, first for Two Higgs Doublet Models (THDM) then for several MSSM scenarios, will be discussed in the next sections.

2.1 Constraints in THDM

We first consider the Two-Higgs Doublet model, in which the SM Higgs sector is extended by the addition of an extra Higgs doublet. Let us consider the four Z_2 symmetric types of the THDM, for which the charged Higgs couplings are given in Table 2, where $\tan\beta$ is the ratio of the VEV's of the two Higgs doublets.

Type	λ_{UU}	λ_{DD}	λ_{LL}
I	$\cot\beta$	$\cot\beta$	$\cot\beta$
II	$\cot\beta$	$-\tan\beta$	$-\tan\beta$
III	$\cot\beta$	$-\tan\beta$	$\cot\beta$
IV	$\cot\beta$	$\cot\beta$	$-\tan\beta$

Table 2: Yukawa couplings for the four types of THDM. U, D and L stand respectively for the up-type quarks, the down-type quarks and the leptons.

As can be seen from the table, at large $\tan\beta$ the charged Higgs strongly couples to the down-type quarks in the THDM types II and III, and to the charged leptons in the THDM types II and IV. For small $\tan\beta$, the situation is reversed, and the couplings to up-type quarks is enhanced in all scenarios.

To study the effect of flavour observables on the THDM models we generate the mass spectra and couplings with 2HDMC [7] and compute the flavour observables with SuperIso v3.4 [6, 8]. The flavour constraints are presented in Fig. 1. In Types II and III, where the charged Higgs coupling to the bottom quarks is enhanced in the large $\tan\beta$ regime and the coupling to the top quarks

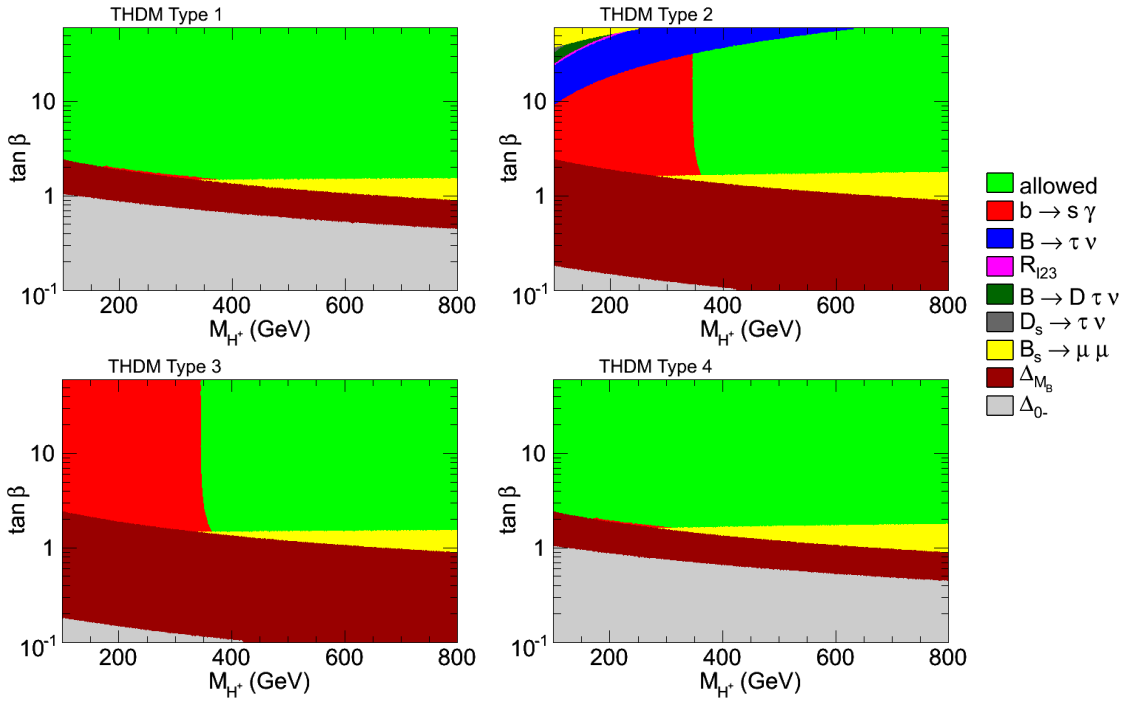

Figure 1: Flavour constraints in THDM types I–IV in the $(M_{H^+}, \tan\beta)$ parameter plane.

is increased at low $\tan\beta$, the SM Wilson coefficients receive a constructive corrections from the charged Higgs loops, resulting in a strong limit from BR($B \to X_s\gamma$) which excludes $M_{H^{\pm}} \lesssim 340$ GeV at 95% C.L. independent of the value of $\tan\beta$.

In addition, in Type II, since both the couplings to bottom quarks and charged leptons are enhanced at large $\tan\beta$, severe constraints can be obtained by several observables such as BR($B_s \to \mu^+\mu^-$) and BR($B_u \to \tau\nu_\tau$). In this case, the charged Higgs corrections result in a decrease in BR($B_u \to \tau\nu_\tau$), while light neutral Higgs bosons generate enhancements proportional to $\tan^4\beta/M_A^4$ in BR($B_s \to \mu^+\mu^-$).

In all scenarios, for low values of $\tan\beta$, the couplings to top quarks is increased, and we see that values of $\tan\beta$ smaller than 2 are excluded by several observables enhanced by charged Higgs-top loops: BR($b \to s\gamma$), $\Delta_0(B \to K^*\gamma)$, ΔM_{B_d} and now even BR($B_s \to \mu^+\mu^-$).

2.2 Constraints in CMSSM

The Constrained MSSM is among the most studied SUSY scenarios. The Higgs sector of the MSSM is similar to the THDM and contains two Higgs doublets, and the couplings of the charged Higgs boson are the same as the ones of the THDM Type II, with enhancements for the down-type quarks and charged leptons. However, large corrections can be induced by the presence of supersymmetric particles in the intermediate states. The most constraining observables are BR($B \to X_s\gamma$), BR($B_s \to \mu^+\mu^-$) and BR($B_u \to \tau\nu$). In addition to the charged Higgs contributions, BR($B \to X_s\gamma$) receives corrections from chargino-squark loops which can add constructively or destructively. BR($B_s \to \mu^+\mu^-$) receives corrections from the neutral Higgs boson contributions, which can be

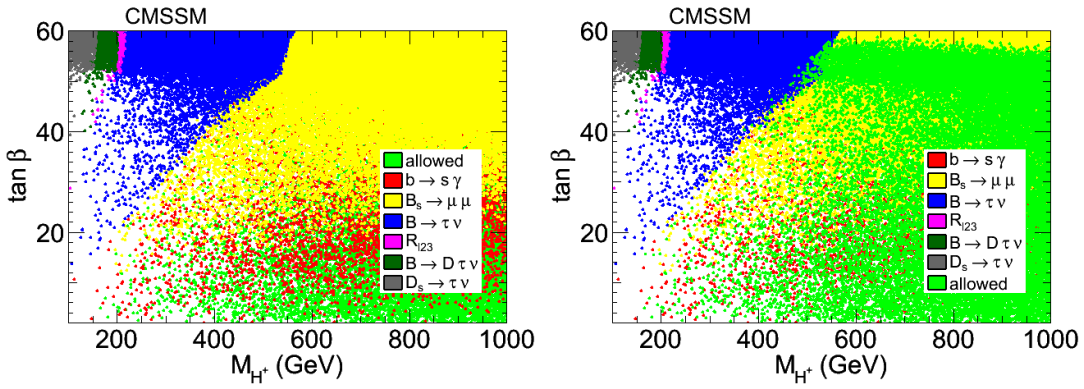

Figure 2: Flavour constraints in the CMSSM, in the $(M_{H^+}, \tan\beta)$ parameter plane, with the allowed (green) points displayed in the background (left) and in the foreground (right).

enhanced by the presence of SUSY particles, resulting in a branching fraction which is proportional to $\tan^6\beta/M_A^4$ in the large $\tan\beta$ limit. As in the THDM Type II, BR($B_u \to \tau\nu$) is sensitive to the charged Higgs boson. The Δ_b corrections can also modify the results.

To study the CMSSM parameter space, we scan over the m_0, $m_{1/2}$, A_0 and $\tan\beta$ parameters, for both signs of μ. We generate the CMSSM mass spectra and couplings with SOFTSUSY [9] and compute the flavour observables with SuperIso v3.4 [6, 8]. As can be seen in Fig. 2, where the results are projected in the $(M_{H^+}, \tan\beta)$ parameter plane, the BR($B \to X_s\gamma$), BR($B_s \to \mu^+\mu^-$) and BR($B_u \to \tau\nu$) provide important constraints. BR($B \to X_s\gamma$) is less sensitive to $\tan\beta$ as compared to the leptonic B decays, and as a result a light charged Higgs is still allowed at small $\tan\beta$. However, these points are disfavoured once the neutral Higgs searches constraints are taken into account.

2.3 Constraints in NUHM

The NUHM model is very similar to the CMSSM, but the universality assumptions are relaxed in the Higgs/Higgsino sector, and two extra parameters, namely the CP-odd Higgs mass M_A (or alternatively $M_{H^\pm}$) and the μ parameter can freely vary. The results in this model are different due to the fact that the charged Higgs mass can be considered as a free parameter. To study this scenario, we scan over the m_0, $m_{1/2}$, A_0, μ, M_A and $\tan\beta$ parameters. We generate the mass spectra and couplings with SOFTSUSY [9] and compute the flavour observables with SuperIso v3.4 [6, 8]. The results are presented in Fig. 3. As expected, the NUHM parameter space enables to probe regions not accessible in the CMSSM, such as the small $M_{H^\pm}$ and $\tan\beta$ region.

2.4 Constraints in pMSSM

We turn now to the phenomenological MSSM, which is the most general CP- and R-parity conserving unconstrained MSSM scenario with 19 parameters [10]. For this study, we scan over the ranges of the pMSSM parameters given in Table 3, generate the pMSSM mass spectra and couplings with SOFTSUSY [9] and compute the flavour observables with SuperIso v3.4 [6, 8].

We have seen that for the CMSSM and NUHM scenarios, BR($B_s \to \mu^+\mu^-$) is the most constraining observable at large $\tan\beta$. We will concentrate here on the effect of the recent ev-

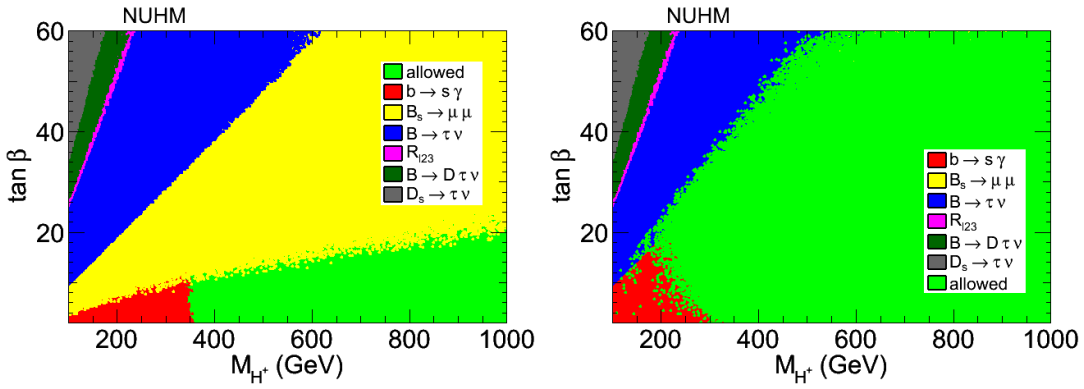

Figure 3: Flavour constraints in NUHM, in the $(M_{H^+}, \tan\beta)$ parameter plane, with the allowed (green) points displayed in the background (left) and in the foreground (right).

Parameter	Range	Parameter	Range
$\tan\beta$	[1, 60]	$M_{\tilde{e}_L} = M_{\tilde{\mu}_L}$	[50, 2500]
M_A	[50, 2000]	$M_{\tilde{e}_R} = M_{\tilde{\mu}_R}$	[50, 2500]
M_1	[-2500, 2500]	$M_{\tilde{\tau}_L}$	[50, 2500]
M_2	[-2500, 2500]	$M_{\tilde{\tau}_R}$	[50, 2500]
M_3	[50, 2500]	$M_{\tilde{q}_{1L}} = M_{\tilde{q}_{2L}}$	[50, 2500]
$A_d = A_s = A_b$	[-10000, 10000]	$M_{\tilde{q}_{3L}}$	[50, 2500]
$A_u = A_c = A_t$	[-10000, 10000]	$M_{\tilde{u}_R} = M_{\tilde{c}_R}$	[50, 2500]
$A_e = A_\mu = A_\tau$	[-10000, 10000]	$M_{\tilde{t}_R}$	[50, 2500]
μ	[-1000, 2000]	$M_{\tilde{d}_R} = M_{\tilde{s}_R}$	[50, 2500]
		$M_{\tilde{b}_R}$	[50, 2500]

Table 3: SUSY parameter ranges (in GeV when applicable).

idence for $B_s \to \mu^+\mu^-$ by LHCb on the pMSSM scenario. The impact of the present and future determinations of this branching ratio on the M_A and $\tan\beta$ parameters is shown in Fig. 4, where we present all the accepted pMSSM points from our scan, the points compatible with the 2011 CMS+LHCb combination, and the ones in agreement with the prospective limit $\mathrm{BR}(B_s \to \mu^+\mu^-) = (3.4 \pm 0.7) \times 10^{-9}$. As expected $\mathrm{BR}(B_s \to \mu^+\mu^-)$ probes the small M_A (or $M_{H^\pm}$) and large $\tan\beta$ region. We also note that this observable is quite sensitive to the other SUSY parameters, and many points can still survive even at large $\tan\beta$.

Combining this constraint with those from dark matter direct detection and from heavy Higgs searches can help exclude the remaining points at large $\tan\beta$ as we will see in the next sections.

3. Dark matter sector

The dark matter problem is a cosmological and astrophysical problem which appears at different scales and is revealed in particular in the WMAP data. It is established that dark matter has to

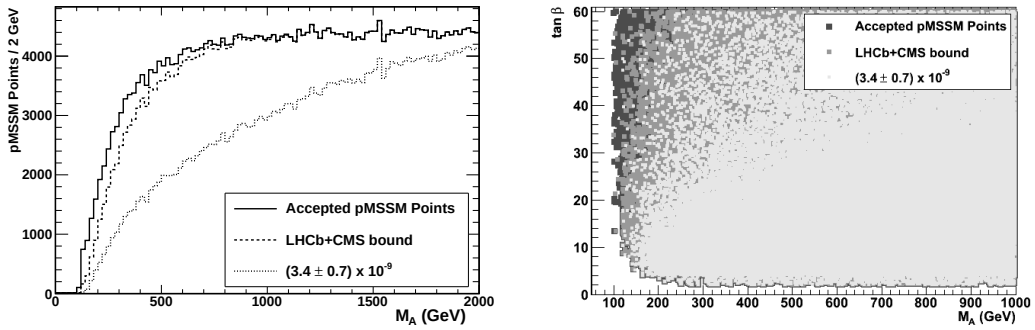

Figure 4: Distribution of pMSSM points after the $B_s \to \mu^+\mu^-$ constraint projected on the M_A (left) and $(M_A, \tan\beta)$ plane (right) for all accepted pMSSM points (medium grey), points not excluded by the combination of the present LHCb and CMS analyses (dark grey) and the projection for the points compatible with the measurement of the SM expected branching fractions with a 20% total uncertainty (light grey).

be cold (*i.e.* with small velocities), and therefore is made of heavy WIMP particles. In the R-parity conserving MSSM, the lightest supersymmetric particle (LSP) is stable and constitute a viable dark matter candidate. In particular, the lightest neutralino is an excellent candidate for dark matter, and in the following, we consider the pMSSM scenario with neutralino LSP.

Dark matter can be probed in different ways. First, direct searches at the LHC, for example through monojet or monophoton final states, or new particles together with missing E_T in the final states, could reveal a manifestation of potential dark matter candidates.

Second, since dark matter is present in large quantities across the Universe, it is important to look for indirect effects of dark matter annihilation to SM particles. This is the basic principle of indirect detection where one can look for the annihilation products in the cosmic rays, used for example by the AMS and PAMELA experiments. The dark matter annihilation processes are also the basis of the calculation of the dark matter relic density, which can be directly compared to the values of the dark matter abundance measured by cosmological experiments, and in particular WMAP and Planck. It is important to notice that the Higgs sector can play an important role here, since there are possible enhancements of the annihilation cross-sections through Higgs resonances. Nevertheless, it has been shown [11, 12] that many cosmological phenomena can strongly alter the value of the calculated relic density and relax the relic density constraint.

The third way to search for dark matter is to consider dark matter scattering with matter, *i.e.* protons or neutrons. This is the principle of dark matter direct detection experiment. Such scattering is sensitive in particular to the presence of a neutral Higgs which can mediate the scattering, and hence dark matter direct detection can directly probe the Higgs sector of the MSSM. The Higgs data and the direct dark matter searches are now starting to probe the bulk of the region of the neutralino-nucleon scattering cross section predicted by the MSSM. In particular, the latest results reported by the XENON collaboration improved the earlier 95% C.L. limit by a factor of ~ 4.

We compare the new XENON limit with the predicted spin–independent χ–p cross sections as a function of the LSP mass for the points fulfilling various selections in Figure 5. The XENON limit removes 28% of the accepted MSSM points before the constraints from the LHC Higgs results

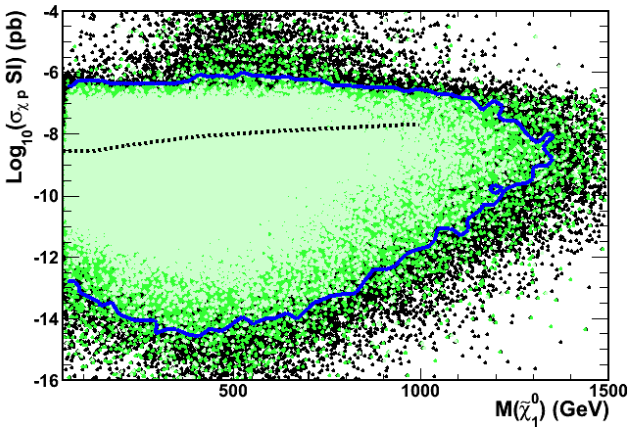

Figure 5: χ-p scattering cross section as a function of the χ_1^0 mass. The black dots represent valid pMSSM points, the dark grey dots the subset of points compatible at 90% C.L. with the LHC Higgs results and the light grey dots compatible at 68% C.L. The region enclosed by the blue continuous line contains 99.5% of the points compatible at 90% C.L. with the LHC Higgs results. The dashed line represents the 95% C.L. upper limit contour set by the XENON100 experiment using 225 live days of data.

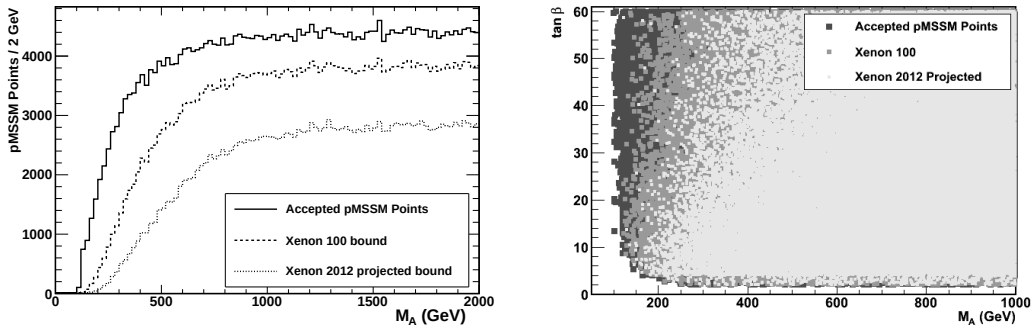

Figure 6: Distribution of pMSSM points after the dark matter direct detection constraint projected on the M_A (left) and $(M_A, \tan\beta)$ plane (right) for all accepted pMSSM points (medium grey), points not excluded by the 2011 XENON-100 data (dark grey) and the 2012 data (light grey).

are applied. This fraction decreases to 24% and 15% when we restrict to the points compatible with the measured Higgs mass and rates at, respectively, the 90% and 68% C.L. This indicates that the pMSSM points favoured by the LHC Higgs results, tend to have a lower χ–p scattering cross section, as a result of the large value of M_A that they imply.

This is confirmed in Fig. 6 where we present the XENON-100 exclusion as functions of M_A and $\tan\beta$. A comparison with Fig. 4 shows that dark matter direct detection probes the same region which is also constrained by $\mathrm{BR}(B_s \to \mu^+\mu^-)$. Combining both constraints is therefore important since it can help exclude points which could pass each constraint separately.

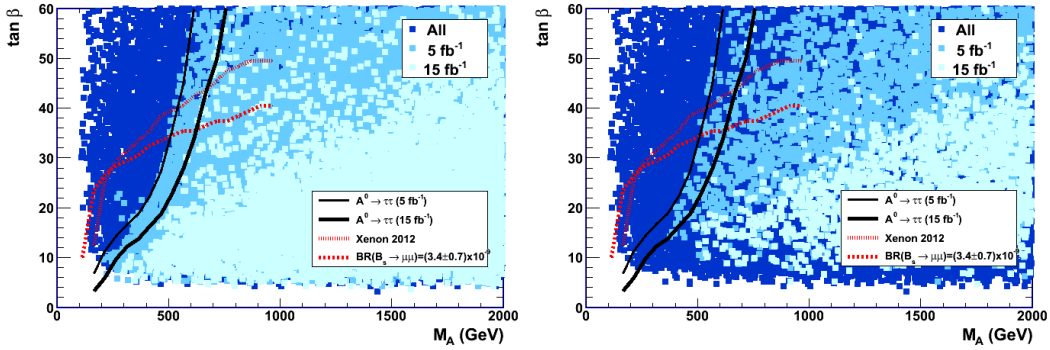

Figure 7: On the left, pMSSM points in the $(M_A, \tan\beta)$, giving $123 < M_h < 129$ GeV. The different shades of blue show all the valid pMSSM points without cuts (dark blue) and those fulfilling the Higgs mass cut allowed by the 2011 data (medium blue) and by the 2012 data (light blue), assuming no signal beyond the lightest Higgs boson is observed. The lines show the regions which include 90% of the scan points for the $A \to \tau^+\tau^-$ and $B_s \to \mu^+\mu^-$ decays at the LHC and the dark matter direct detection at the XENON experiment. In the right, the points also fulfil constraints from the Higgs rate measurements.

4. Combined constraints

In this section, we analyse the results when combining the different constraints at hand. We compute the flavour observables and relic density with SuperIso Relic [13], the supersymmetric particle decay rates with `SDECAY` [14] and we use `PYTHIA 6` [15] for event generation of inclusive SUSY production in pp interactions. The generated events are then passed through fast detector simulation using `Delphes` [16]. The Higgs decay rates are computed with `HDECAY` [17]. More details can be found in [18, 19, 20].

The results of the direct searches for the light and heavy Higgs bosons at the LHC constitute a very important piece of information on the $(M_A, \tan\beta)$ plane. The determination of the mass of the lightest Higgs boson places some significant constraints on the SUSY parameters. In order to evaluate these constraints, we select the accepted pMSSM points from our scans, which have $122 < M_h < 129$ GeV and have a relic density consistent with the WMAP upper bound. These are $\sim 20\%$ of the points not already excluded by the LHC SUSY searches in our scan, where parameters are varied in the range given in Table 3.

Figure 7 shows the points fulfilling these conditions, which are also allowed by the other 2011 and the 2012 data constraints. We observe that imposing the value of M_h selects a broad wedge in the $(M_A, \tan\beta)$ plane, at rather heavy A masses and moderate to large values of $\tan\beta$ and extending beyond the projected sensitivity of the searches in the $A \to \tau^+\tau^-$ but also that of direct dark matter detection and would be compatible with a SM-like value for the rate of the $B_s \to \mu^+\mu^-$ decay. We also impose in the right plot the condition that the yields in the $\gamma\gamma$, W^+W^- and ZZ final states reproduce the observed rates of candidate events reported by the ATLAS and CMS collaborations at the end of the 7 TeV run. Here, we observe that the wedge in the $(M_A, \tan\beta)$ plane is further restricted and solutions with small M_A (or $M_{H^{\pm}}$) are also strongly suppressed.

5. Conclusions

Until now, direct searches for New Physics at the LHC did not succeed in discovering particles beyond the Standard Model, and as a result the constraints from SUSY searches push the particle masses to larger values. We have shown that constraints from indirect searches in the flavour and dark matter sectors, as well as from Higgs searches, can also provide important constraints on the supersymmetric parameter space, which are complementary to direct SUSY searches. In particular, the large $\tan\beta$ and small M_A or $M_{H^{\pm}}$ region is constrained by several different constraints, favouring a decoupling scenario for the MSSM Higgs bosons.

Acknowledgements

I would like to thank the organisers for their invitation and for the very fruitful workshop. I am also grateful to A. Arbey, M. Battaglia and O. Stål for discussions and collaborations.

References

[1] CMS Collaboration, CMS-PAS-SUS-12-016.

[2] ATLAS Collaboration, ATLAS-CONF-2012-109.

[3] R. Aaij *et al.* [LHCb Collaboration], Phys. Rev. Lett. **110** (2013) 021801 [arXiv:1211.2674].

[4] LHCb Collaboration, LHCb-CONF-2012-008.

[5] Y. Amhis *et al.* [Heavy Flavor Averaging Group Collaboration], arXiv:1207.1158 [hep-ex].

[6] F. Mahmoudi, Comput. Phys. Commun. **180** (2009) 1579 [arXiv:0808.3144].

[7] D. Eriksson, J. Rathsman and O. Stal, Comput. Phys. Commun. **181** (2010) 189 [arXiv:0902.0851].

[8] F. Mahmoudi, Comput. Phys. Commun. **178** (2008) 745 [arXiv:0710.2067].

[9] B. C. Allanach, Comput. Phys. Commun. **143** (2002) 305 [hep-ph/0104145].

[10] A. Djouadi *et al.* [MSSM Working Group Collaboration], hep-ph/9901246.

[11] A. Arbey and F. Mahmoudi, Phys. Lett. B **669** (2008) 46 [arXiv:0803.0741].

[12] A. Arbey and F. Mahmoudi, JHEP **1005** (2010) 051 [arXiv:0906.0368].

[13] A. Arbey and F. Mahmoudi, Comput. Phys. Commun. **181** (2010) 1277 [arXiv:0906.0369].

[14] M. Muhlleitner, A. Djouadi and Y. Mambrini, Comput. Phys. Commun. **168** (2005) 46 [hep-ph/0311167].

[15] T. Sjostrand, S. Mrenna and P. Z. Skands, JHEP **0605** (2006) 026 [hep-ph/0603175].

[16] S. Ovyn, X. Rouby and V. Lemaitre, arXiv:0903.2225 [hep-ph].

[17] A. Djouadi, J. Kalinowski and M. Spira, Comput. Phys. Commun. **108** (1998) 56 [hep-ph/9704448].

[18] A. Arbey, M. Battaglia and F. Mahmoudi, Eur. Phys. J. C **72** (2012) 1847 [arXiv:1110.3726].

[19] A. Arbey, M. Battaglia and F. Mahmoudi, Eur. Phys. J. C **72** (2012) 1906 [arXiv:1112.3032].

[20] A. Arbey, M. Battaglia, A. Djouadi and F. Mahmoudi, JHEP **1209** (2012) 107 [arXiv:1207.1348].